# Recent progress in characterizing multiscale ionospheric phenomena with GNSS and applications:
# *Solar Flare over-ionization & Medium Scale Travelling Ionospheric Disturbances*

*SGI meeting, TU Berlin, Germany*
*07-08July 2015*

M. Hernández-Pajares[1], E. Monte-Moreno[1], A. García-Rigo [1], H. Yang [1], P. Wielgosz [2], T. Hadasz [3], R. Orus-Pérez[4], R. Prieto-Cerdeira[4], Y. Beniguel[5], T. Singh[6]

[1] UPC-IonSAT/TALP Res. groups, Barcelona, Spain,
[2] UWM, Olzstyn, Poland, [3] WUELS, Wroclaw, Poland, [4] ESA-ESTEC, Noordijk, The Netherlands, [5] IEEA, Paris, France, [6] Indian Institute of Technology (BHU) ,Varanasi, India.
[contact e-mail: manuel@ma4.upc.edu]

# Outline

*1. Ionospheric electron content and GNSS*

*2. Characterizing some of the underlying phenomenae: realistic assumptions on spatial distribution*

*3. Example 1: Solar Flare overionization*

*4. Example 2: Medium Scale Travelling Ionospheric Disturbances*

*5. Conclusions*

# 1) Ionospheric electron content and GNSS

# Ionospheric Electron Content & GNSS

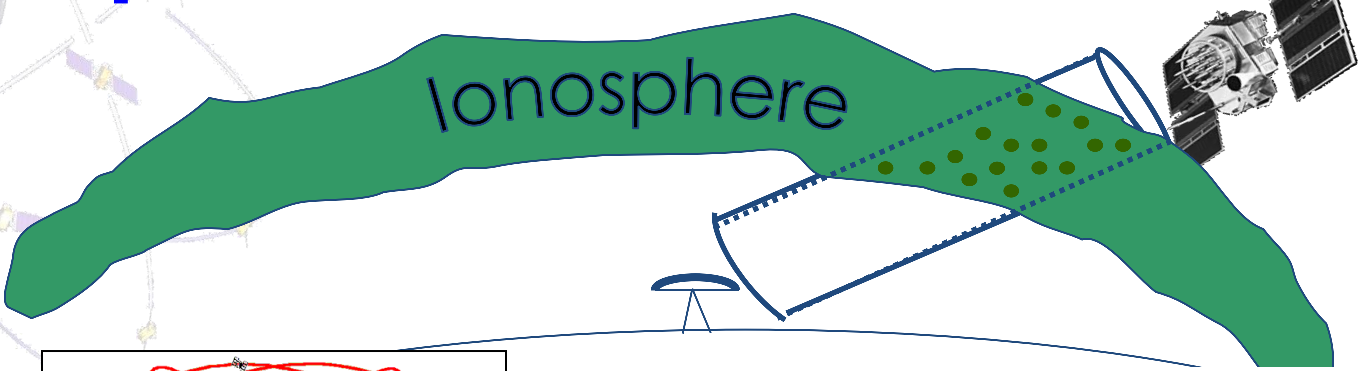


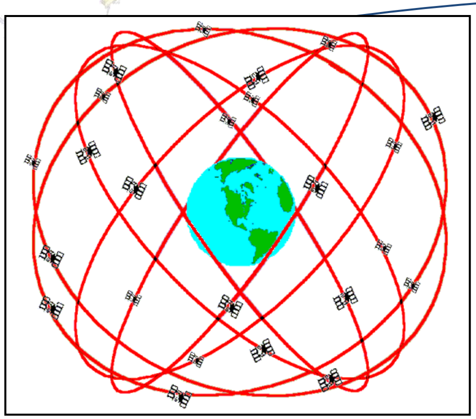

GNSS

Sat. + Rec.

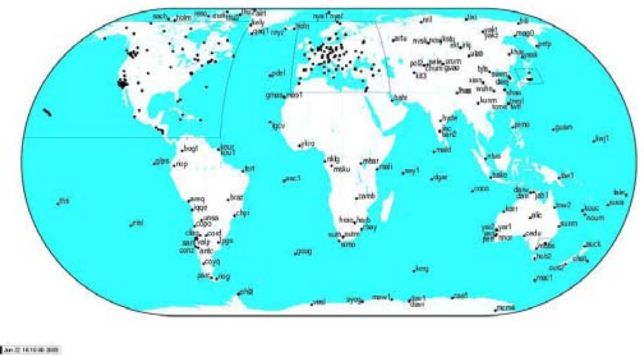

- GNSS iono delay is prop. to Slant Total Electron Content (STEC) & inversely proportional to squared frequency.
- Dual-freq users can cancel out 99.9% of iono delay.
- Dual-freq permanent GNSS nets.: VTEC & Ne for improving single and multi-frequency GNSS precise navigation, Space Weather monitoring, Seismic-related signatures...

# Ionospheric variability at large horizontal and vertical scales

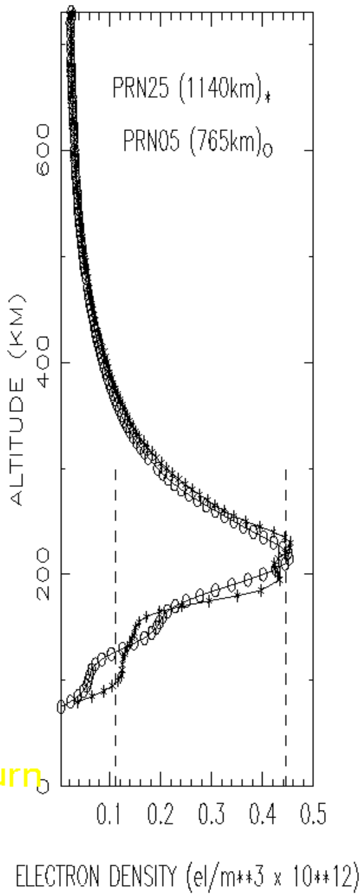


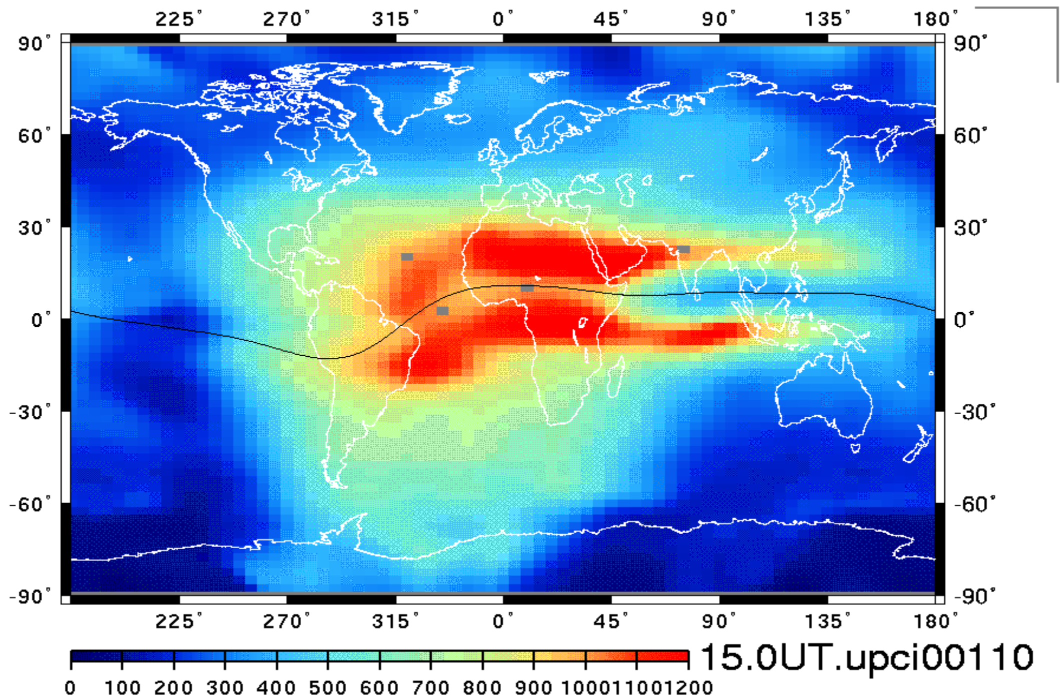


Global Vertical Total Electron Content (VTEC) map computed from ~100 GPS dual-freq CORS (units: 0.1 TECU).

Electron density (Ne) profile computed from LEO GPS data (units: Te-/m**3).

# Ionospheric variability at diff. time scales

## Scintillation

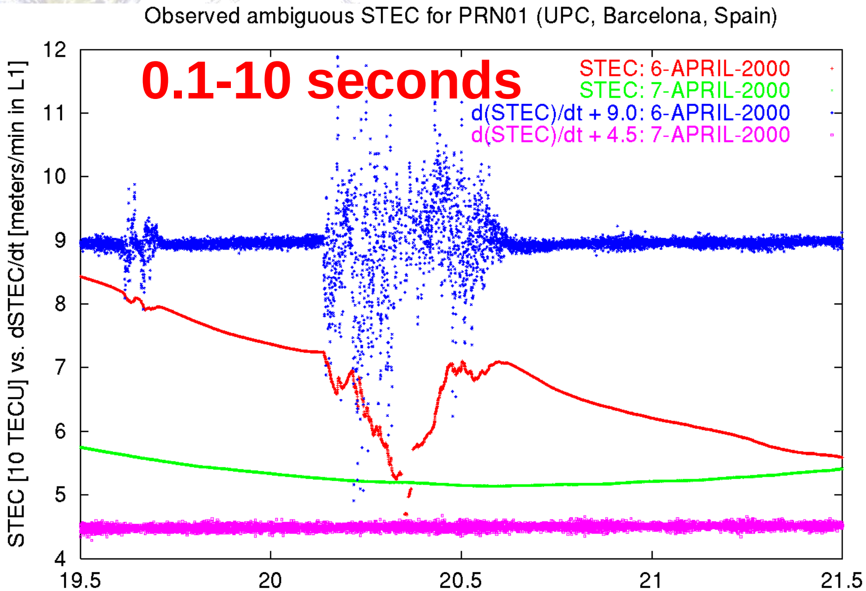


## Solar Flare sudden overioniz.

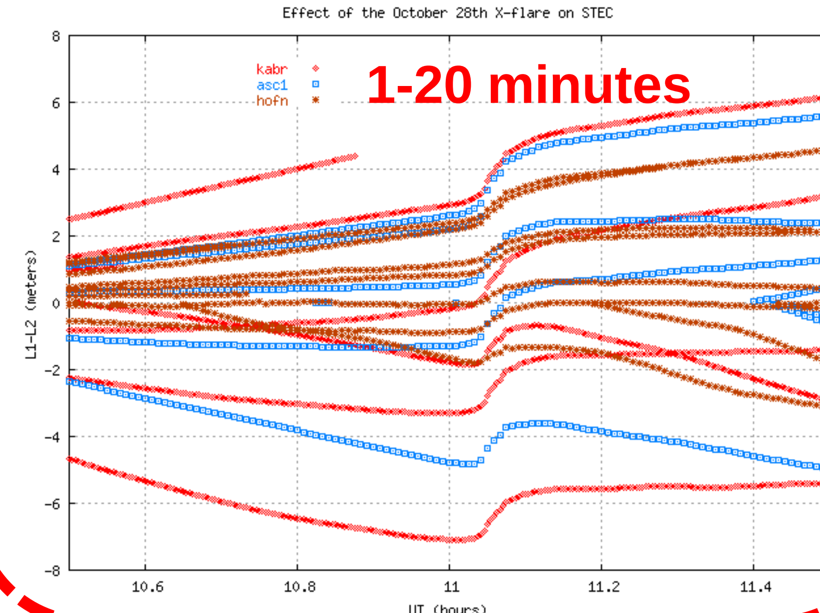


## Travelling Ionospheric Disturb.

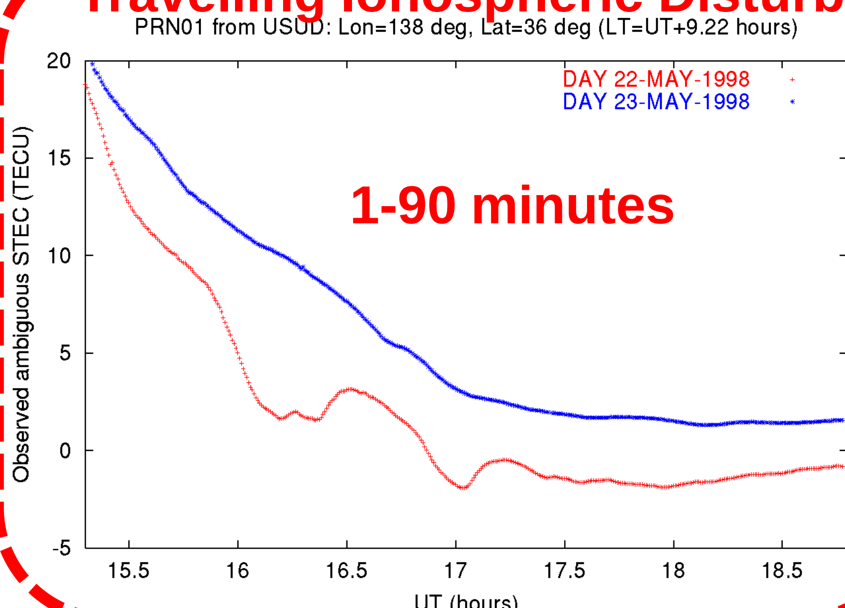


## Solar-cycle,seasonal, solar rot.

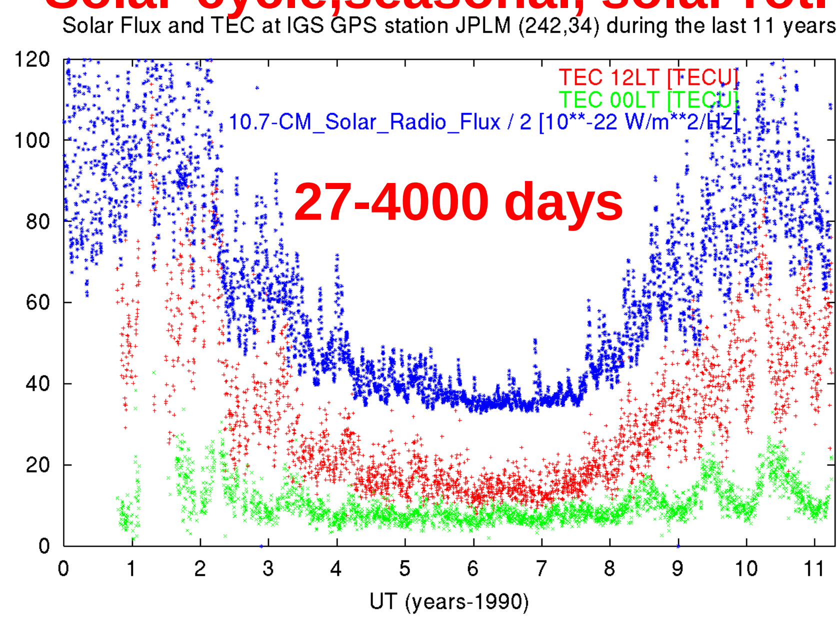

# 3) Characterizing some of the underlying phenomenae by realistic assumptions on spatial distribution

# 3a) Solar Flares

# Global and sudden STEC increase in the day hemisphere due to Solar X-flares

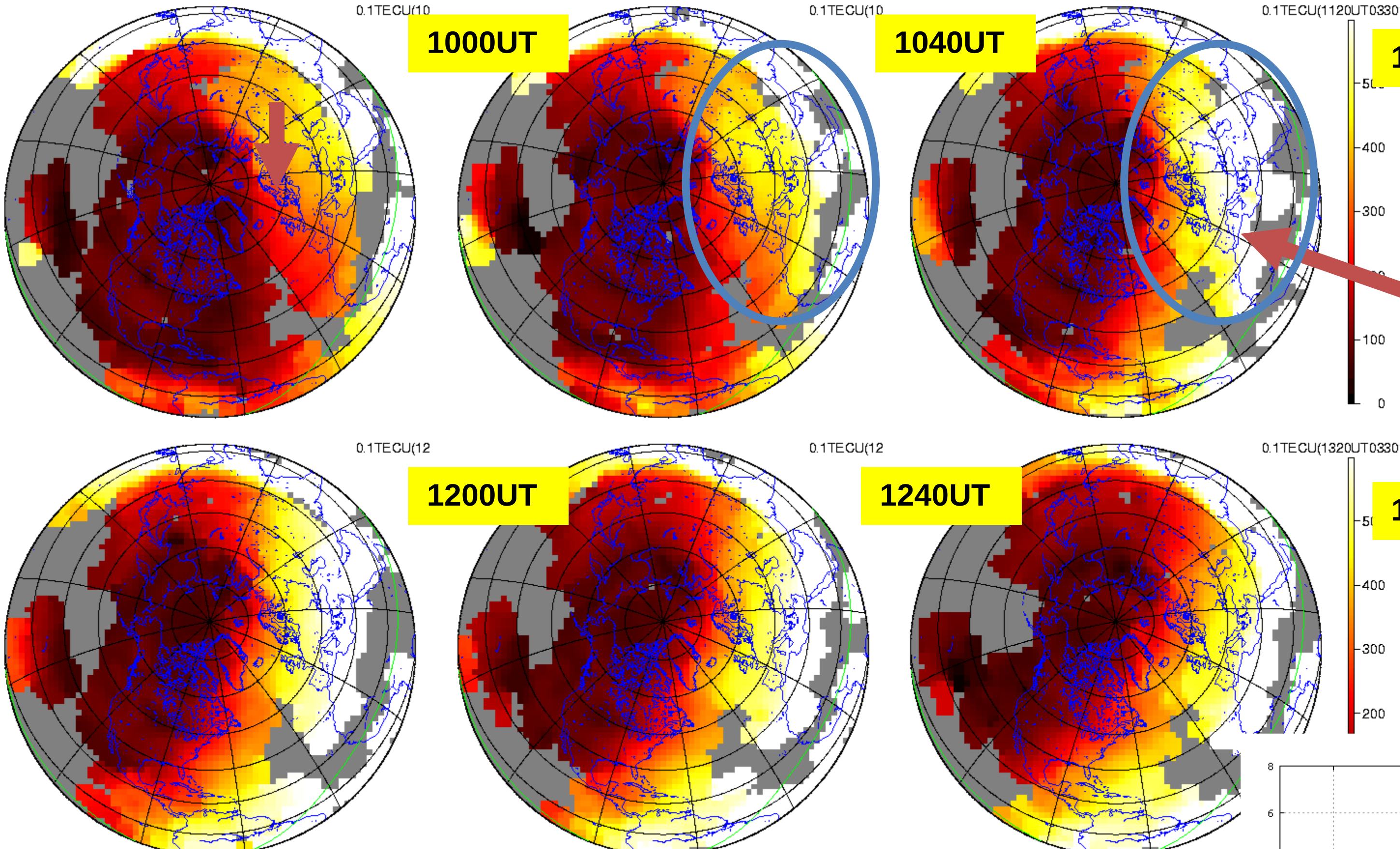


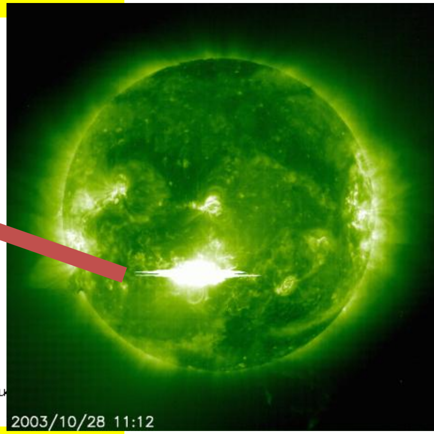


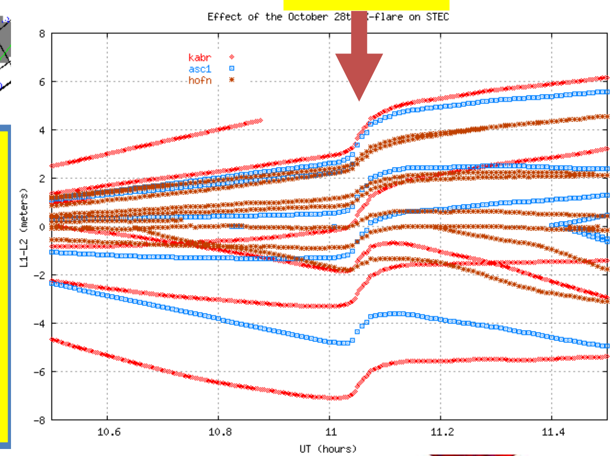


High and sudden STEC variations are experienced in the day hemisphere GPS receivers due to the arrival of the X-rays extra radiation due to Solar X-flares (example: event during 28 Oct. 2003, 11UT approx, preceding the previous mentioned superstorm).

# Recent example: M-class Solar Flare during day 072, 2015 (preceeding St. Patrick's geom. storm)

**VTEC drift rate vs. Latitude**

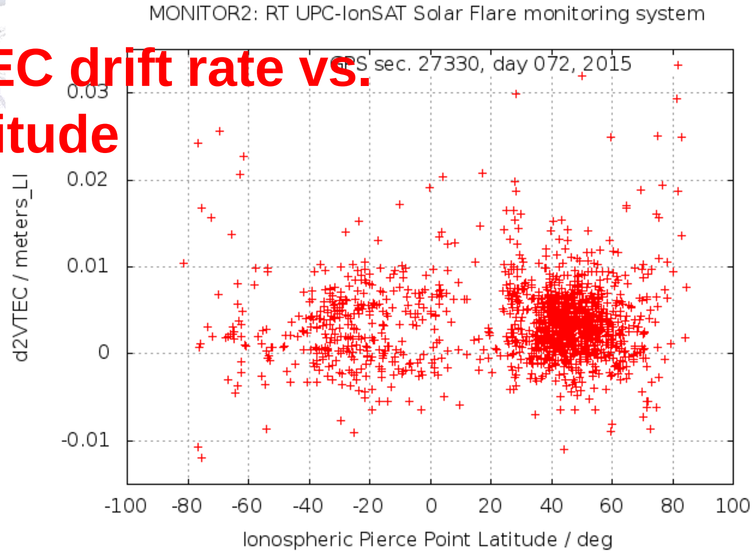


**VTEC drift rate vs. Local Time**

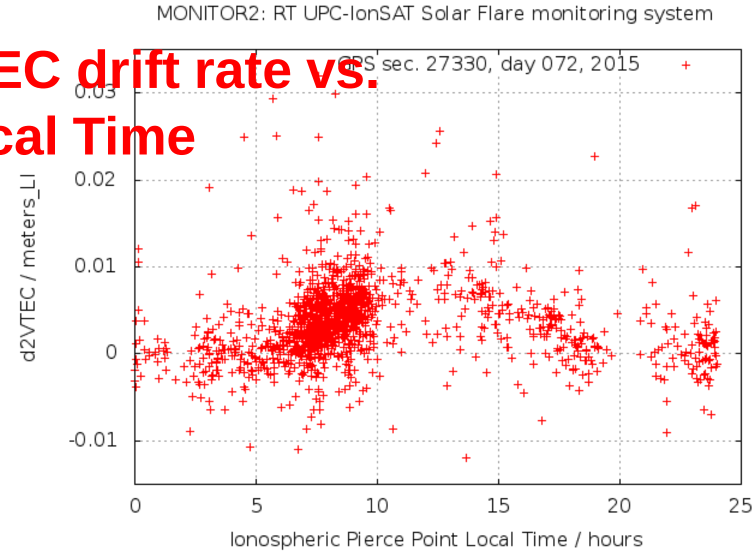


**VTEC drift rate vs. Cosinus of Solar-zenith angle**

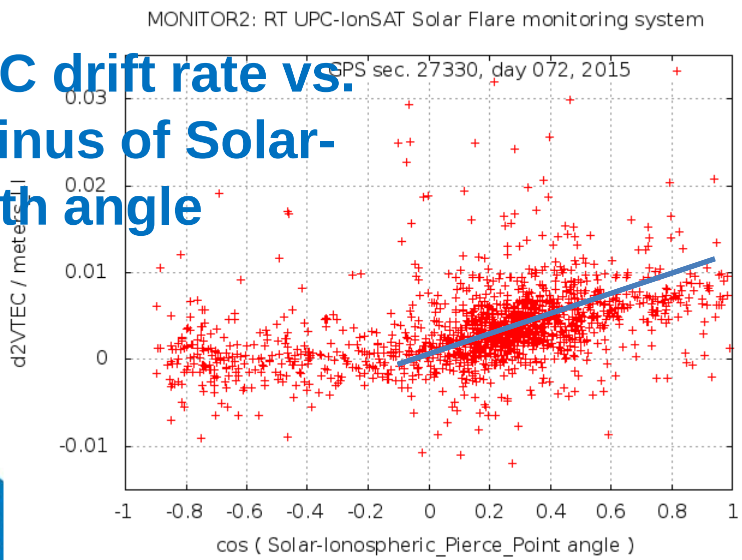


**The slope (GSFLAI) vs. time**

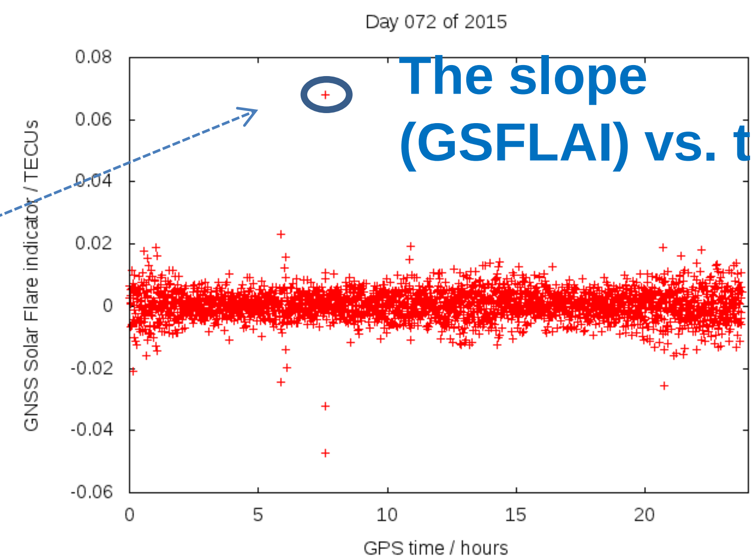

# Overionization model: First principles, GPS… and GSFLAI

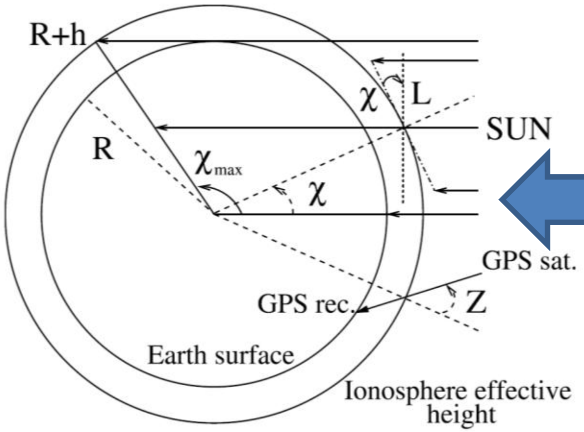


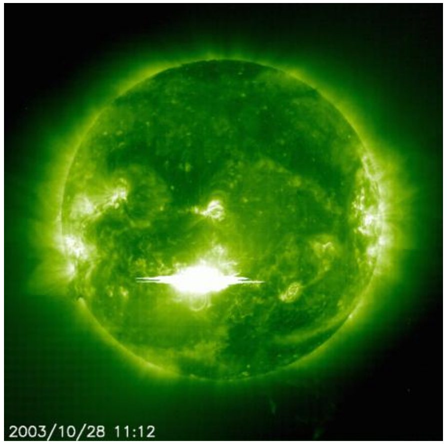


$$\dot{V} = \eta' \cdot C(\chi) \cdot \dot{I}$$

Halloween X-class SF snapshot: **the regresion line slope (GSFLAI)** reacts well.

$$\dot{V} = a_1 \cos\chi + a_2$$

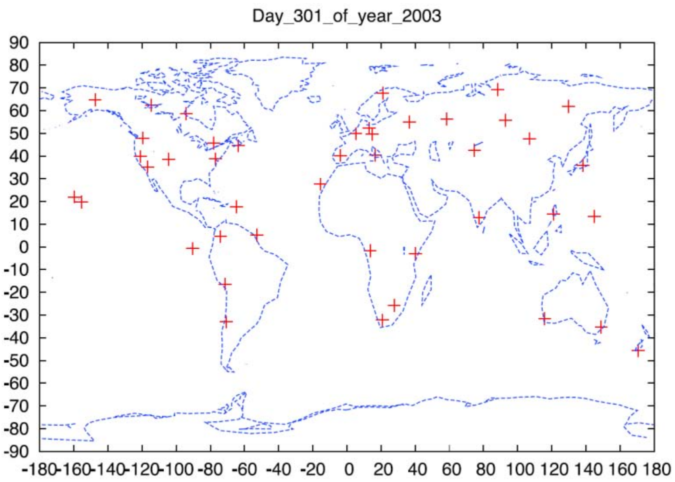


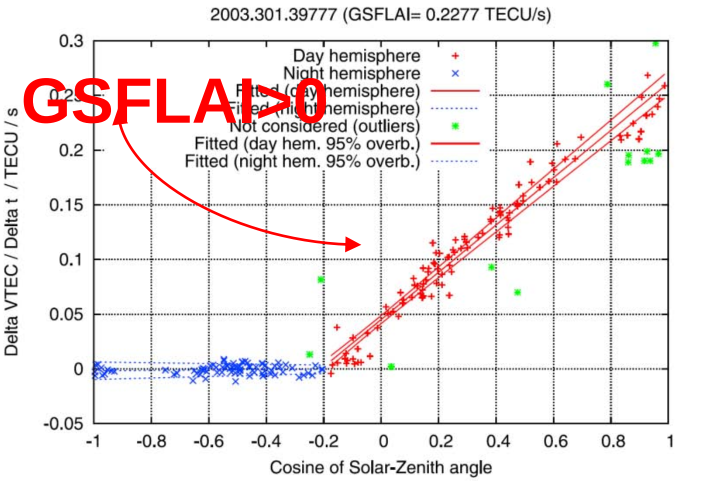


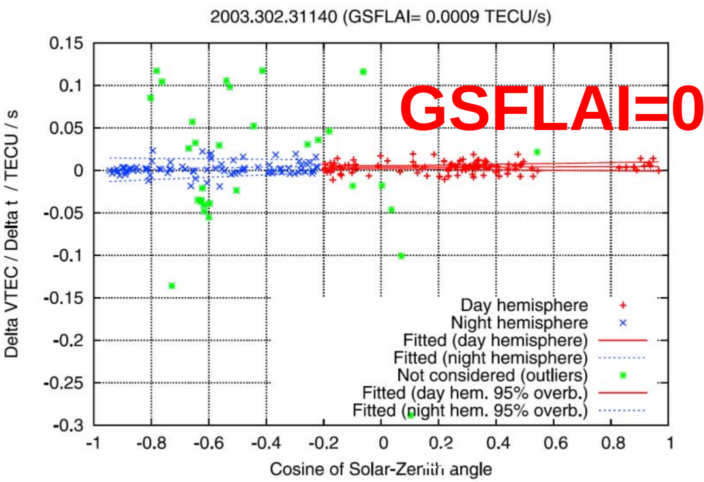


During the next day major geomagnetic storm peak, the higher variations doesn't follow the SF spatial pattern, and GSFLAI (=0) performs again well.

# GSFLAI is a good proxy of direct EUV rate meas., also for M- and C-class Solar Flares

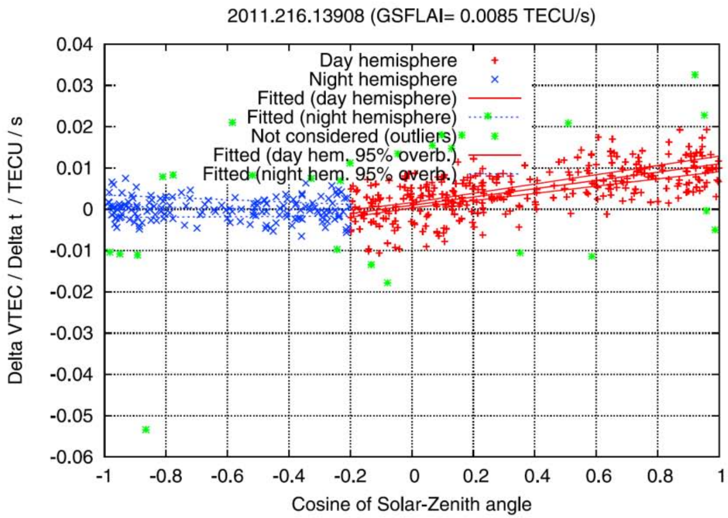


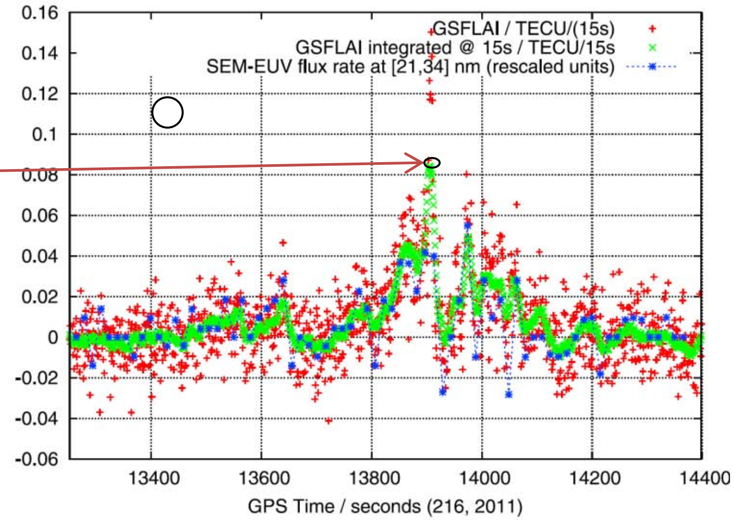


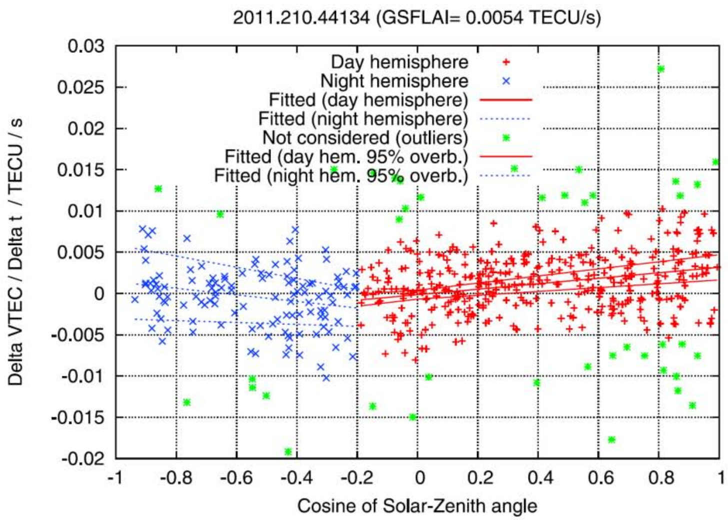


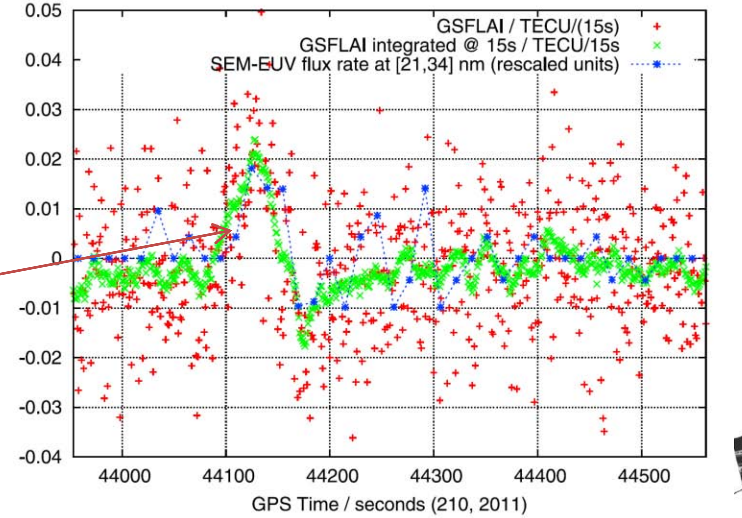

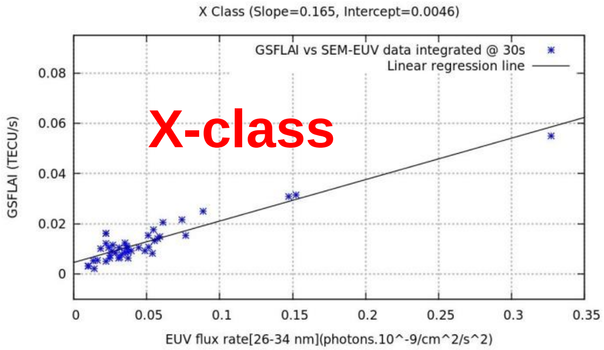


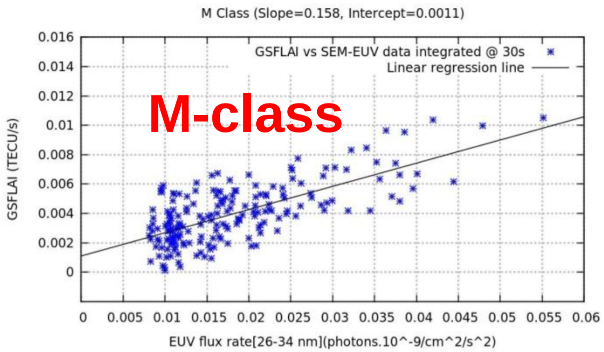


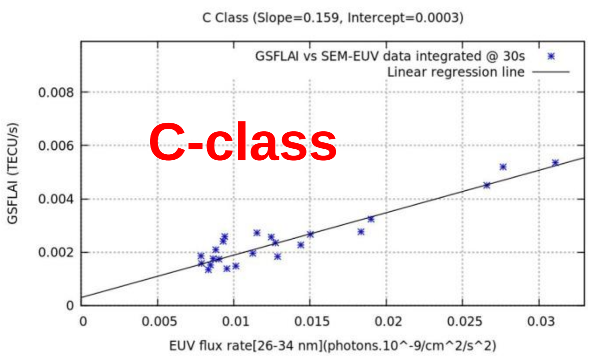


# The GSFLAI, a proxy of EUV flux rate for X, M & C-class S. Flares

- GSFLAI (point with fastest increase per flare, if above the GNSS measurement error) vs. EUV flux rate data (from SOHO-SEM in 26-34 nm range).

- From top to bottom: X, M and C class Solar Flares meeting the criteria since 2001 until 2014.

- Regression lines, with **slopes 0.165, 0.157 and 0.159 for X, M & C-class** => high consistency of the simple physical model & technique.

***Singh et al. (2015), Estimation of Solar EUV ux rate during Strong, Mid and Weak Solar flares using GPS satellite data, in submission to JGR-Space Physics.***

| Flares | | Slope | | Intercept | | Corr. Factor | |
|---|---|---|---|---|---|---|---|
| Class | Number | All | Peaks | All | Peaks | All | Peaks |
| $X$ | 60 | 0.184 | 0.165 | 0.0022 | 0.0046 | 0.83 | 0.94 |
| $M$ | 320 | 0.127 | 0.157 | 0.0012 | 0.0012 | 0.63 | 0.70 |
| $C$ | 300 | 0.111 | 0.159 | 0.0008 | 0.0003 | 0.46 | 0.94 |

[a] The units are $TECU/s$ for GSFLAI and $photons.10^-9/cm^2/s^2$ for EUV flux rate.

# The Solar Flare location distance to the disc center (proximity to limb) matters....

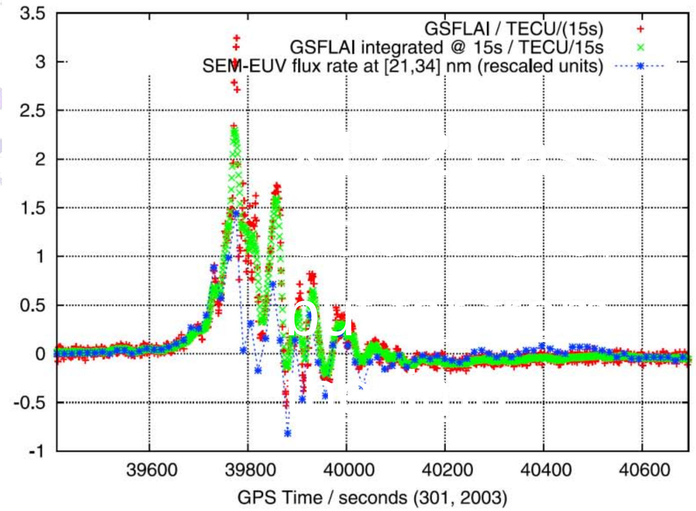


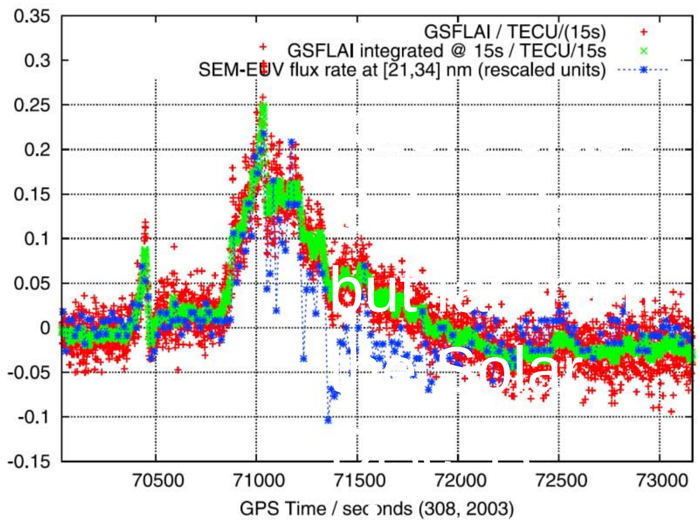


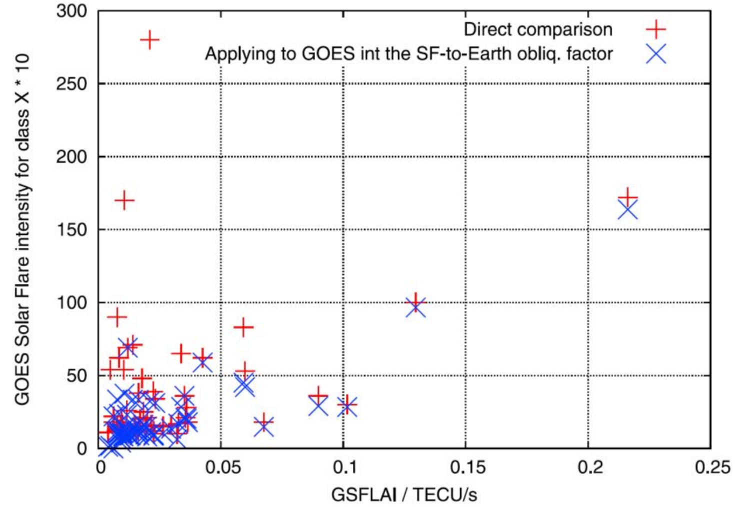


After applying a simple extinction law from Solar disc distance, a relationship of GSFLAI with GOES X-ray based classification is disclosed, making feasible its usage as geophysical index (a potential proxy of GOES classification...).

# Recent findings on Solar Flares by analyzing GSFLAI time series since 2001

- The solar flare time series have extreme properties regarding amplitude and time correlation.

- The fractional Brownian model proposed in

***Monte E., Hernández-Pajares, M. (2014). Occurrence of solar flares viewed with GPS: Statistics and fractal nature, Journal of Geophysical Research: Space Physics, 119, 11, 9216-9227.***

accounts for the probability of the observed extremely high values of the time series, and also with the fact that the flares appear in bursts.

- Another practical consequence is that the statistical characterization done in this paper allows for the estimation of the probability of a given GNSS solar flare indicator value and also the length of a given burst of flares.

- The probability of observing a GNSS solar flare indicator threshold value 2 times greater than the maximum observed one in last solar cycle (Solar flare preceeding the Halloween geomagnetic storm), is once every 44 years approximately.

# 3b) Medium Scale Travelling Ionospheric Disturbances

# MSTIDs

- Medium Scale Travelling Ionospheric Disturbances (MSTIDs) are ionospheric signatures of waves with some potential origins (Solar Terminator, Weather activity, Perkins inst.).
- Up to few TECUs of amplitude (1 TECU ~ 0.16 m  L1).
- MSTIDs propagate equatorward in daytime (autumn & winter) and westward in night-time (spring & summer).
- Typical periods: 500-2000 sec, velocities: 50-400 m/s.

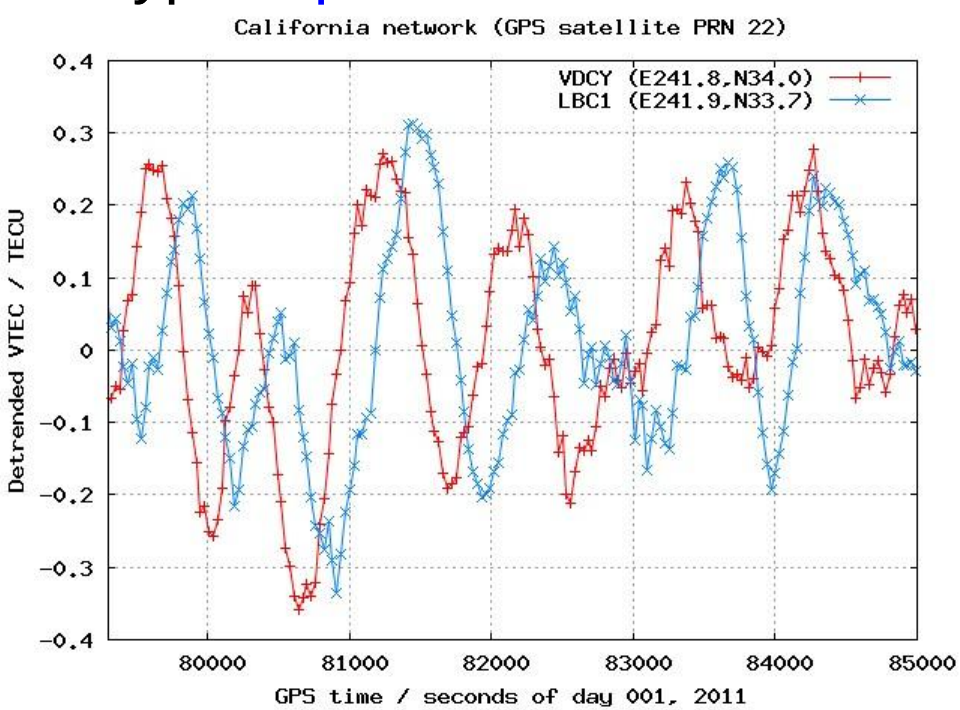


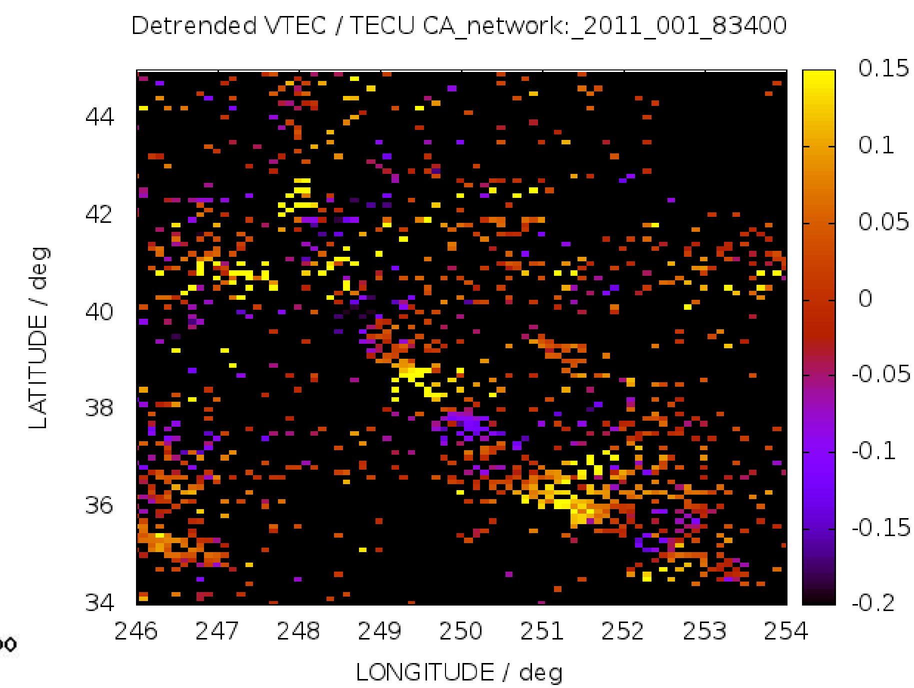

# GNSS ionospheric interferometry scenario

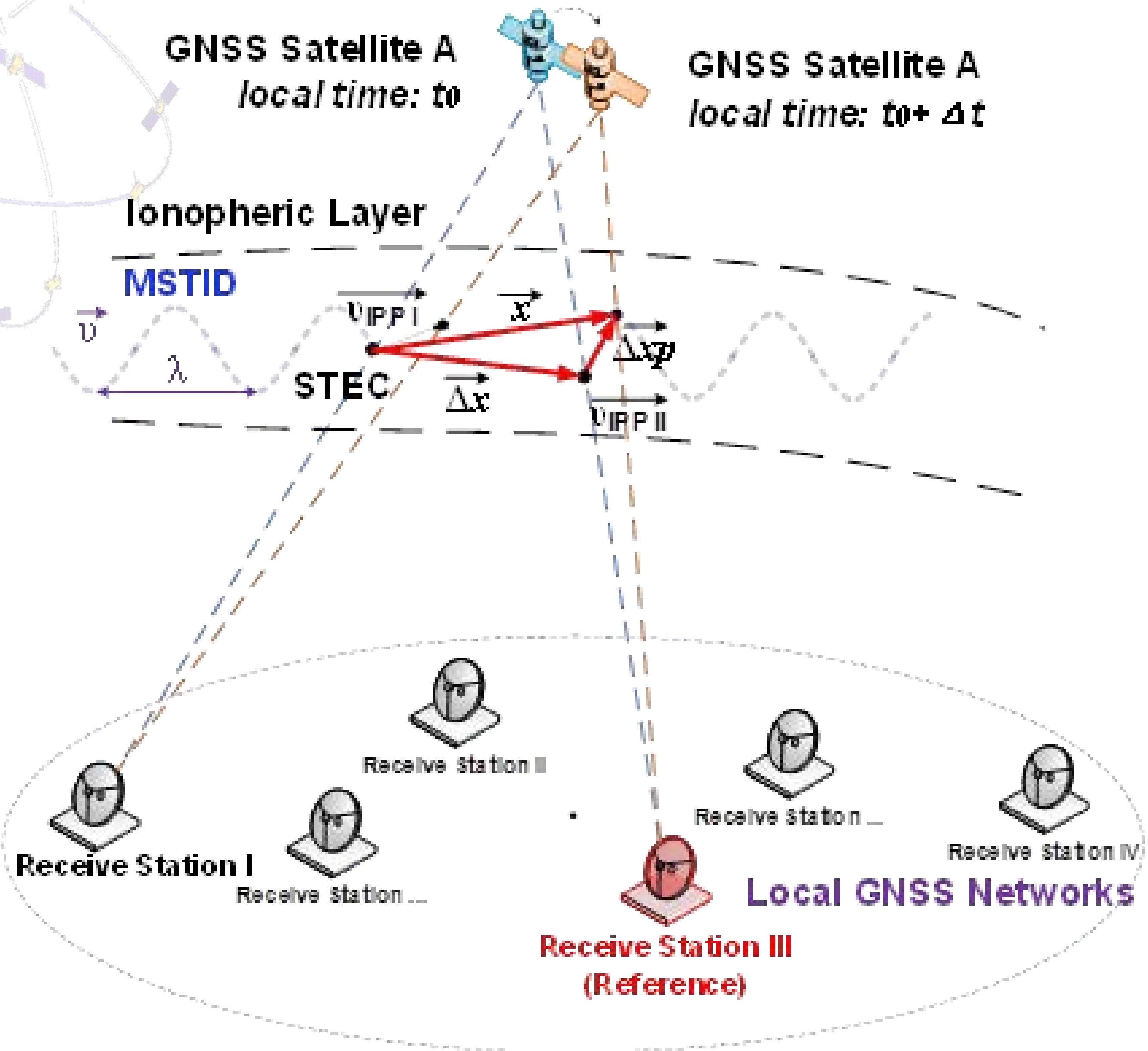

# Rationale of recent MSTID research

**Lack of dense Local GNSS Networks**

*Hernández-Pajares et al. (2015) in prep. for GRL*

**Ambiguity Resolution in GNSS Ionospheric Interferometry (ARGII)**

MSTID vel. est., natural extension to dense networks with diameters $>\lambda_{MSTID}/2 \approx 50$km (comput. burden affordable).

NEW

**Ionospheric Doppler MSTID (IDEM)**

- MSTID vel. est.,
- very simple,
- no distance limitation,
- no large network required (either any receiver can be used for MSTID velocity monitoring elsewhere)

NEW

**Direct GNSS Ionospheric Interfe-rometry (dGII)**

- MSTID vel. no needed, smooth,
- potentially applicable to scales of ~100 km

Improved

*Hernández-Pajares et al. (2015) in prep. for JGR-SP*

**Precise GNSS positioning** (RTK)

**Precise GNSS Troposphere determination**

# Example: Implementation of dGII

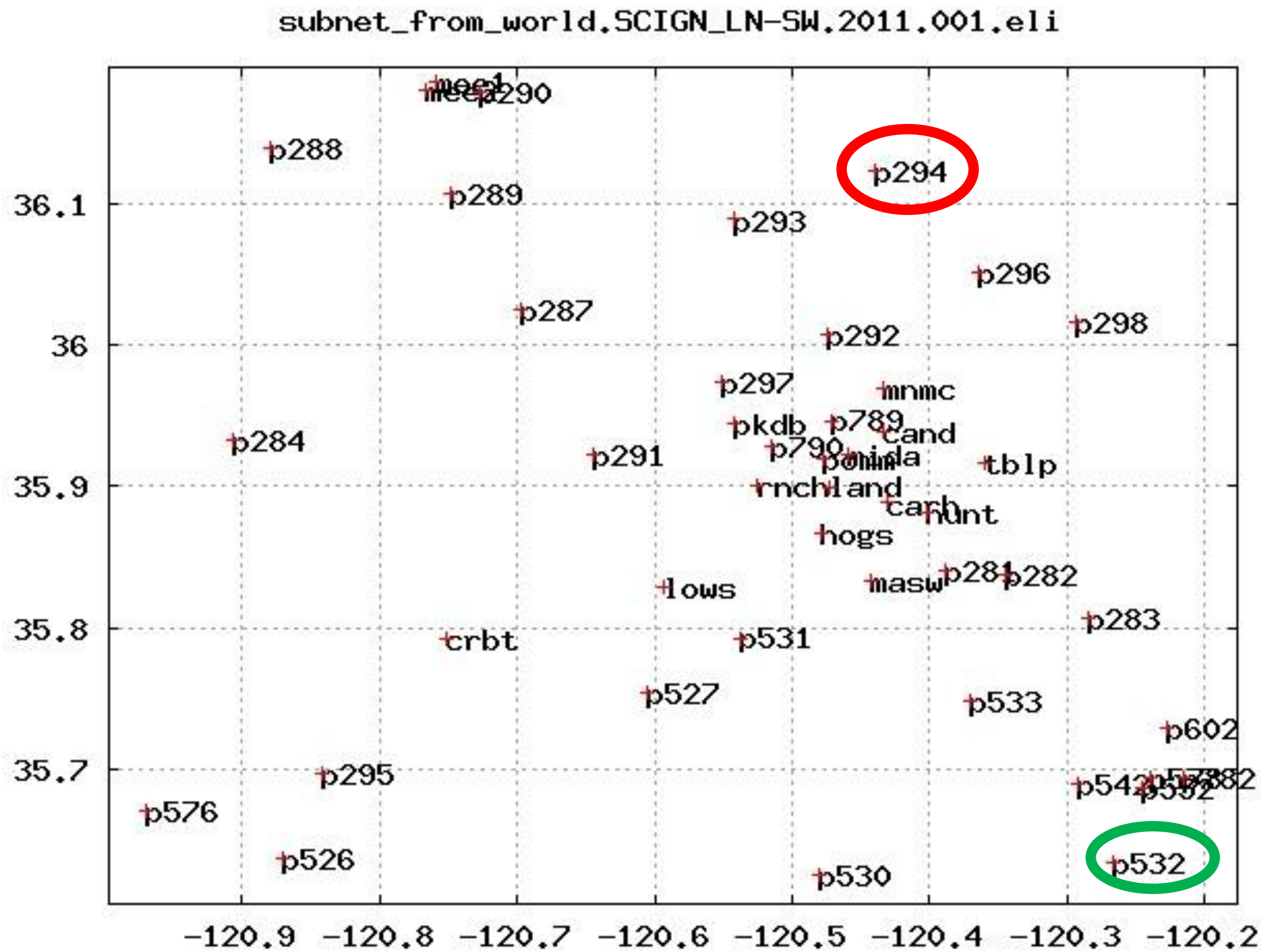

# Example: STEC from LI calibrated with UPC GIM

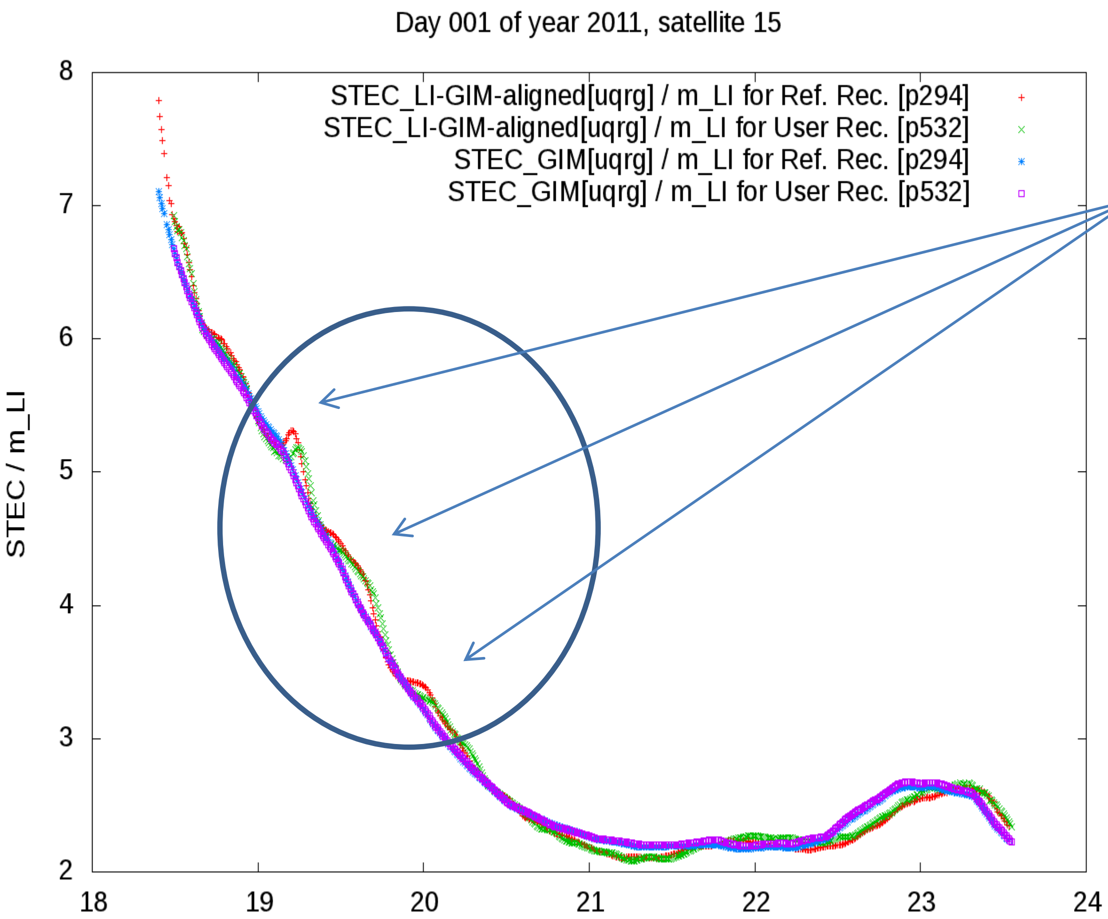


Consistent with measured (and expected, *Hernández-Pajares et al. 2012*) equatorward winter day-time (LT 10.5 to 15.5h) MSTID propagation

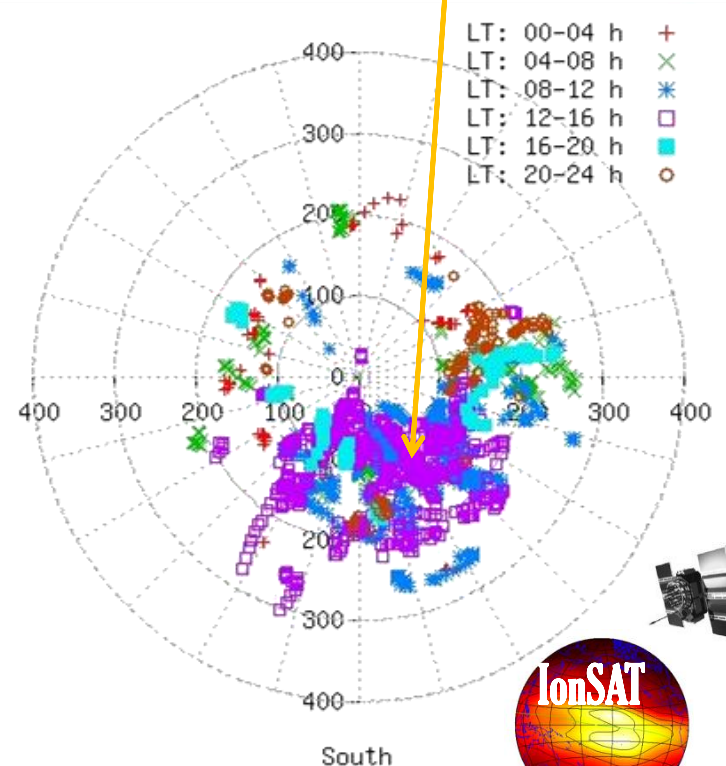

# Example: dVTEC/dt directly observed @ 60 sec

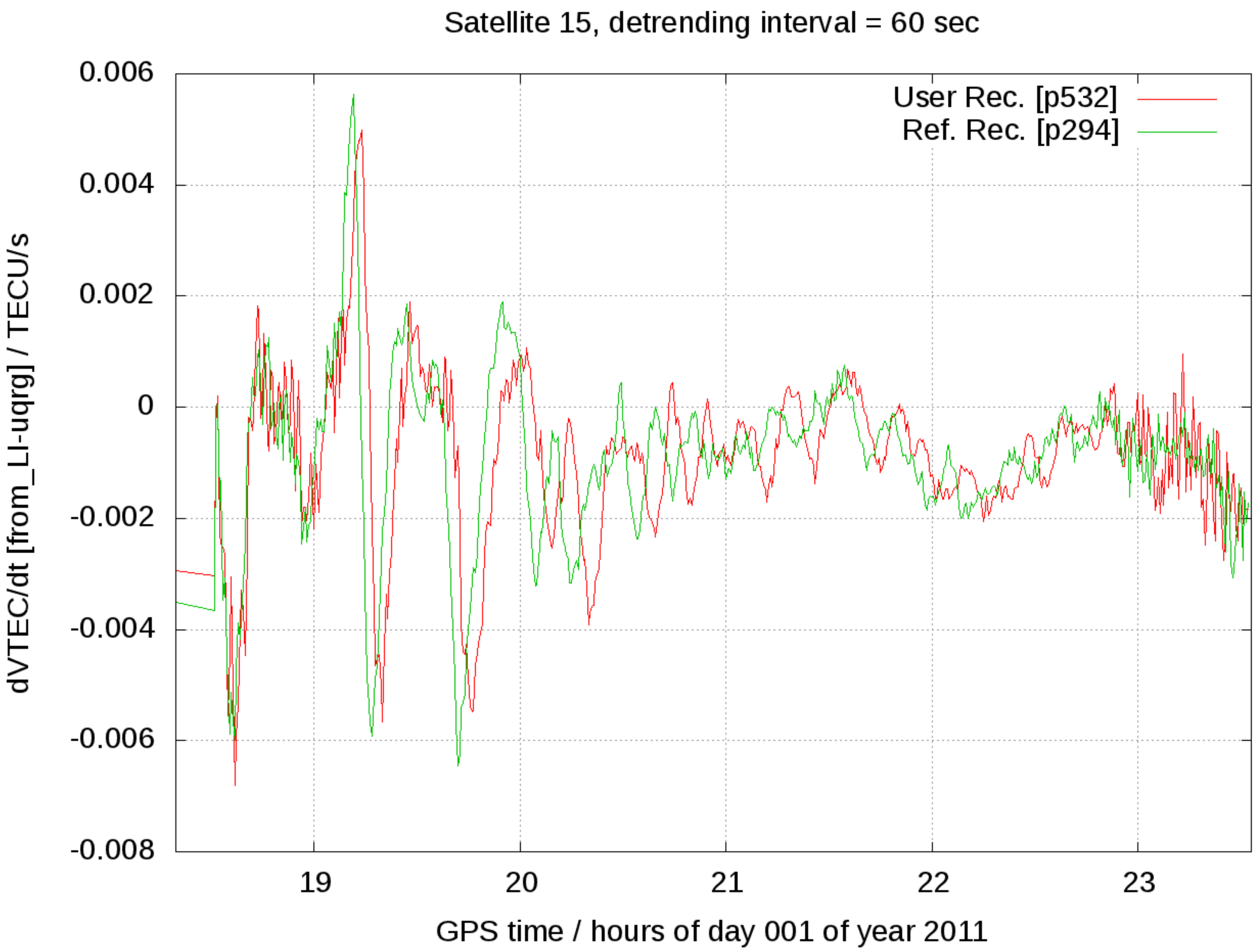

# Example: Significant and dominant MSTID time delay from cross-correlation

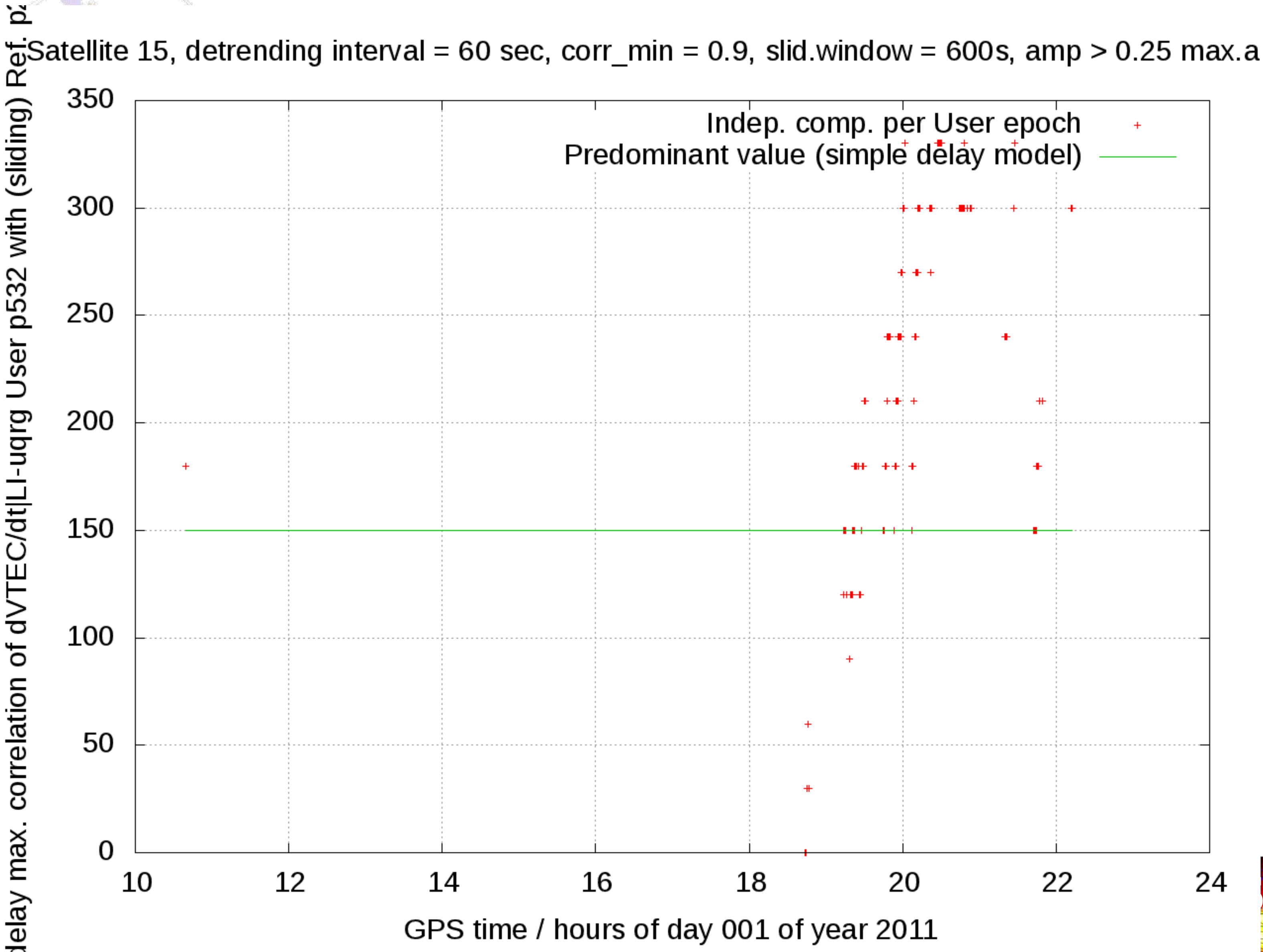

# Example: dVTEC/dt obs, applying predominant MSTID time delay

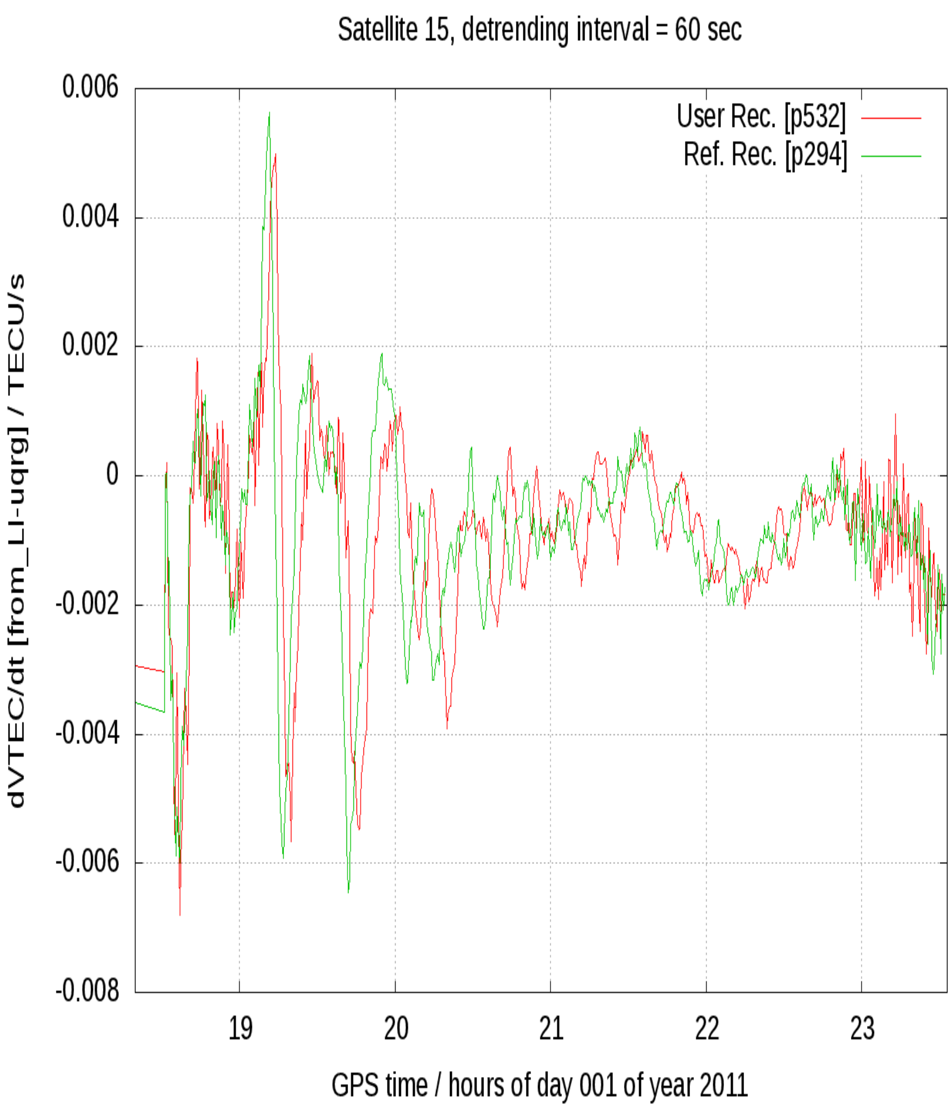


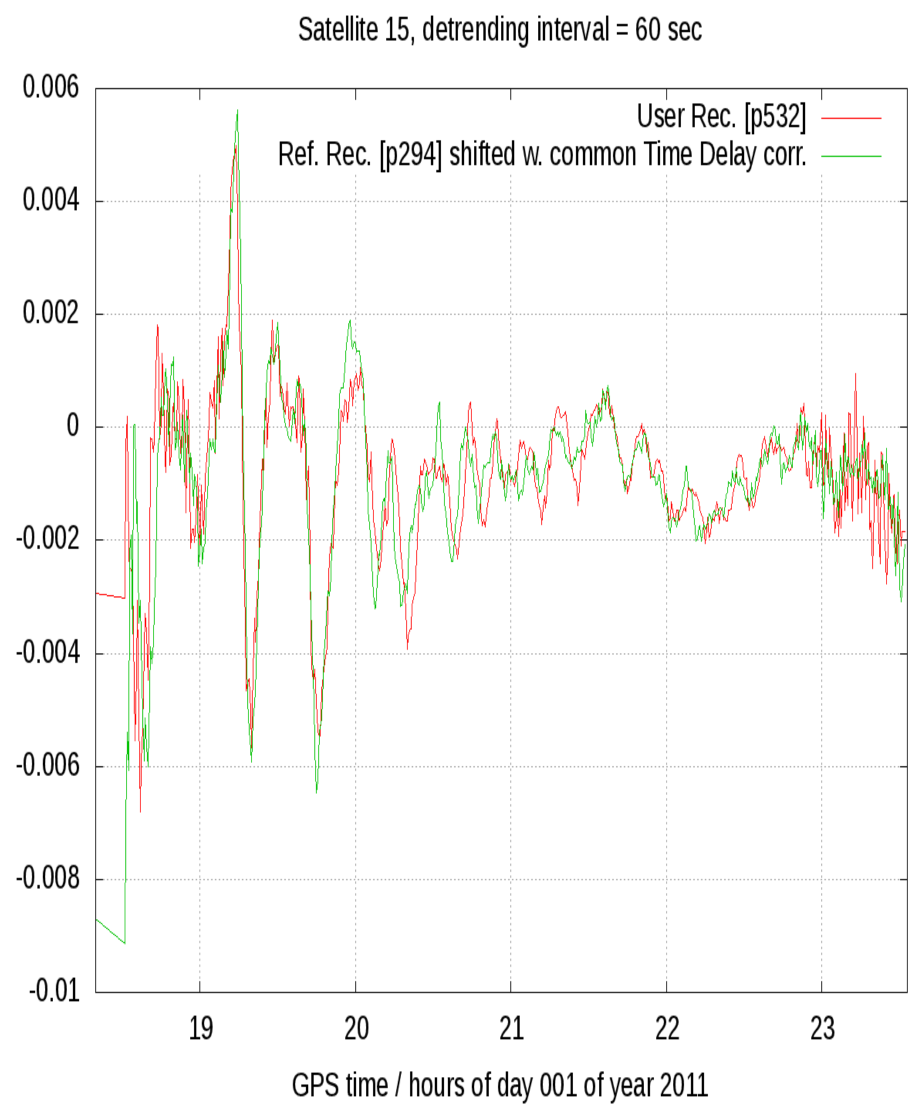

# STEC (from LI calibrated with GIM) after applying pred. MSTID time delay with consistent mapping

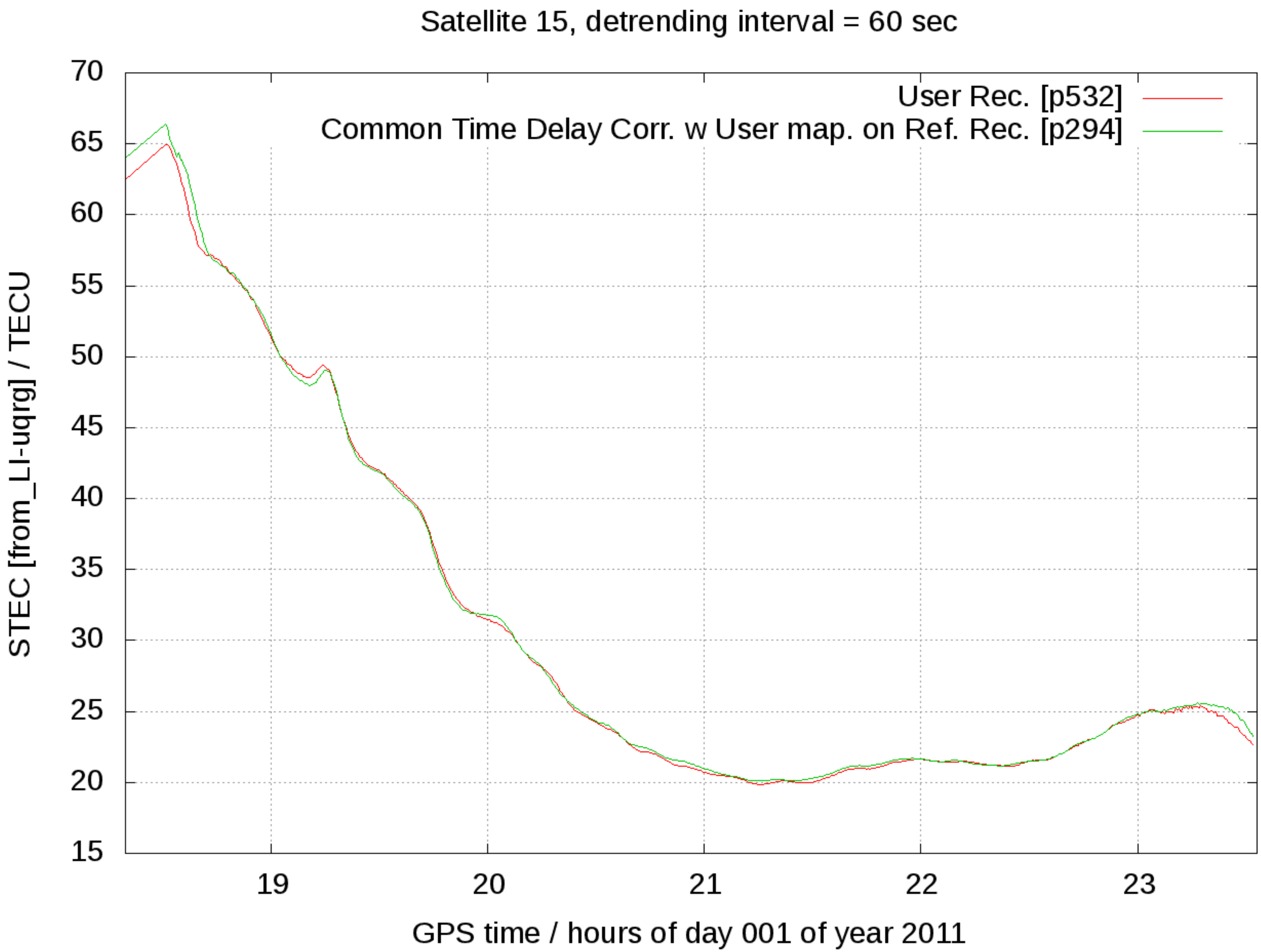

# STEC error with different approaches with consistent mapping

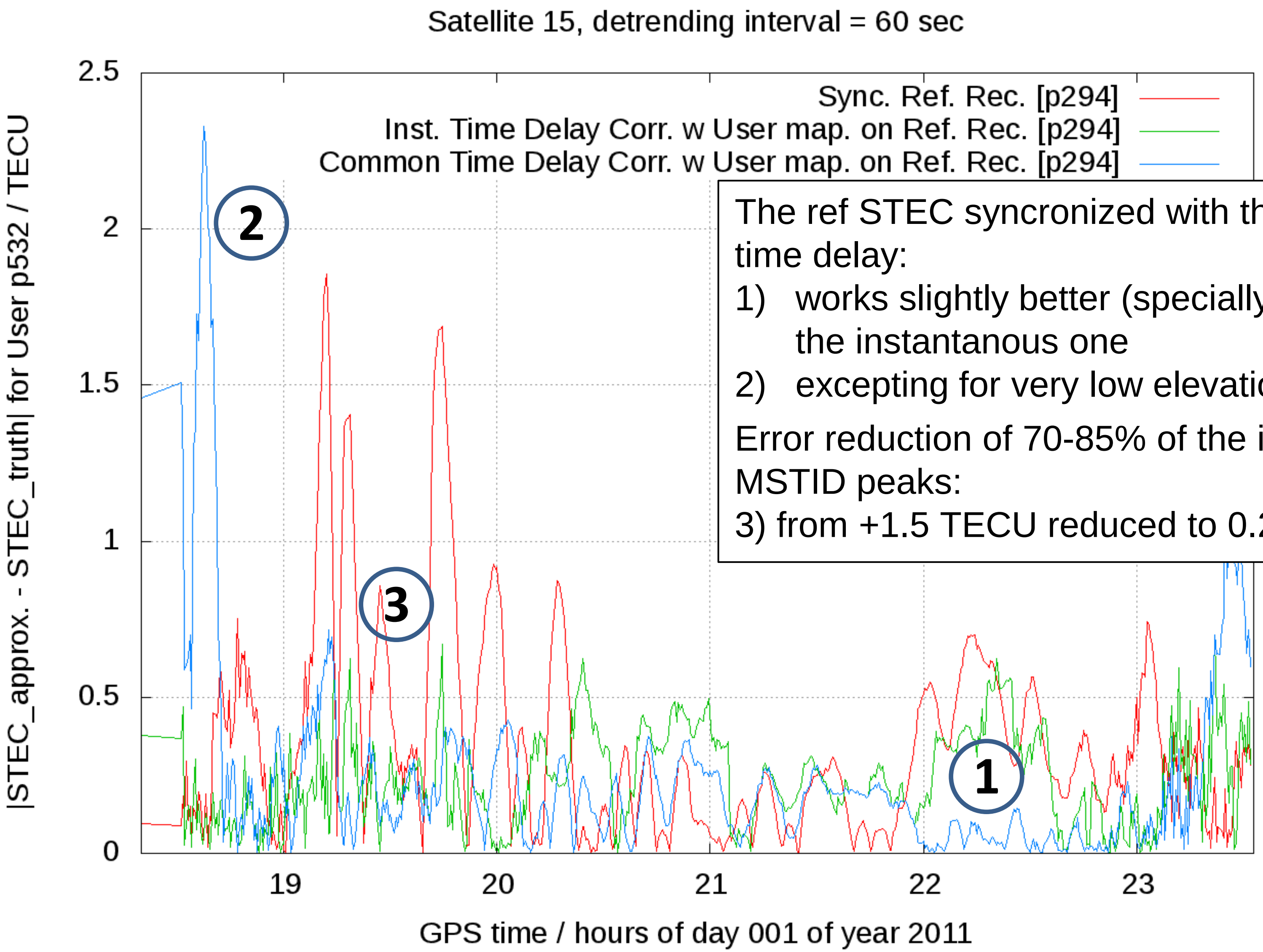


The ref STEC syncronized with the predominant time delay:

1) works slightly better (specially at 22-22.8h) than the instantanous one
2) excepting for very low elevation.

Error reduction of 70-85% of the initial error in MSTID peaks:

3) from +1.5 TECU reduced to 0.2-0.7 TECU.

# Extensive dGII application (range domain): winter day (353,  2014 @ Poland)

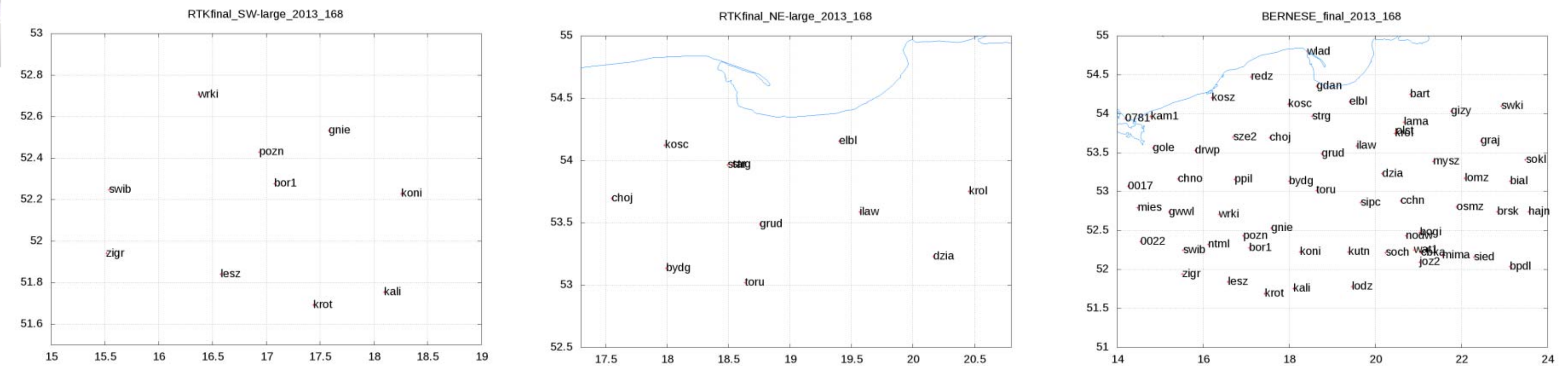


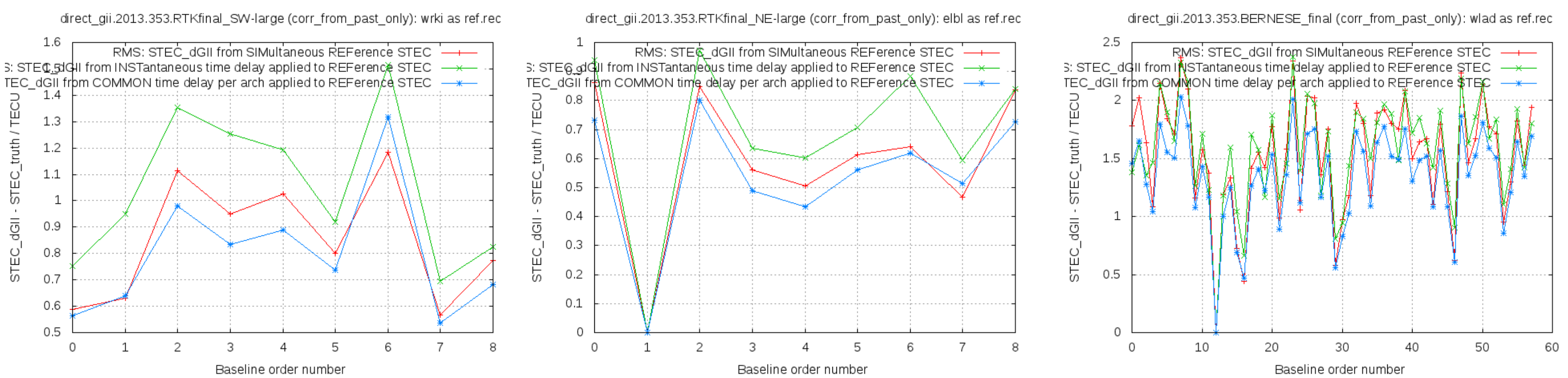


Map of dGII analyzed receivers in RTKfinal-SW-large (left), RTKfinal-NE-large (central) and BERNESE-final networks (right), and corresponding performance of **dGII** for different baselines, **vs. no applying it**, with northern reference sites wrki, elbl and wlad, respectively (right column, Poland, winter day of 353, 2013).

# Extensive dGII application (range domain): summer (168, 2014 @ Poland)

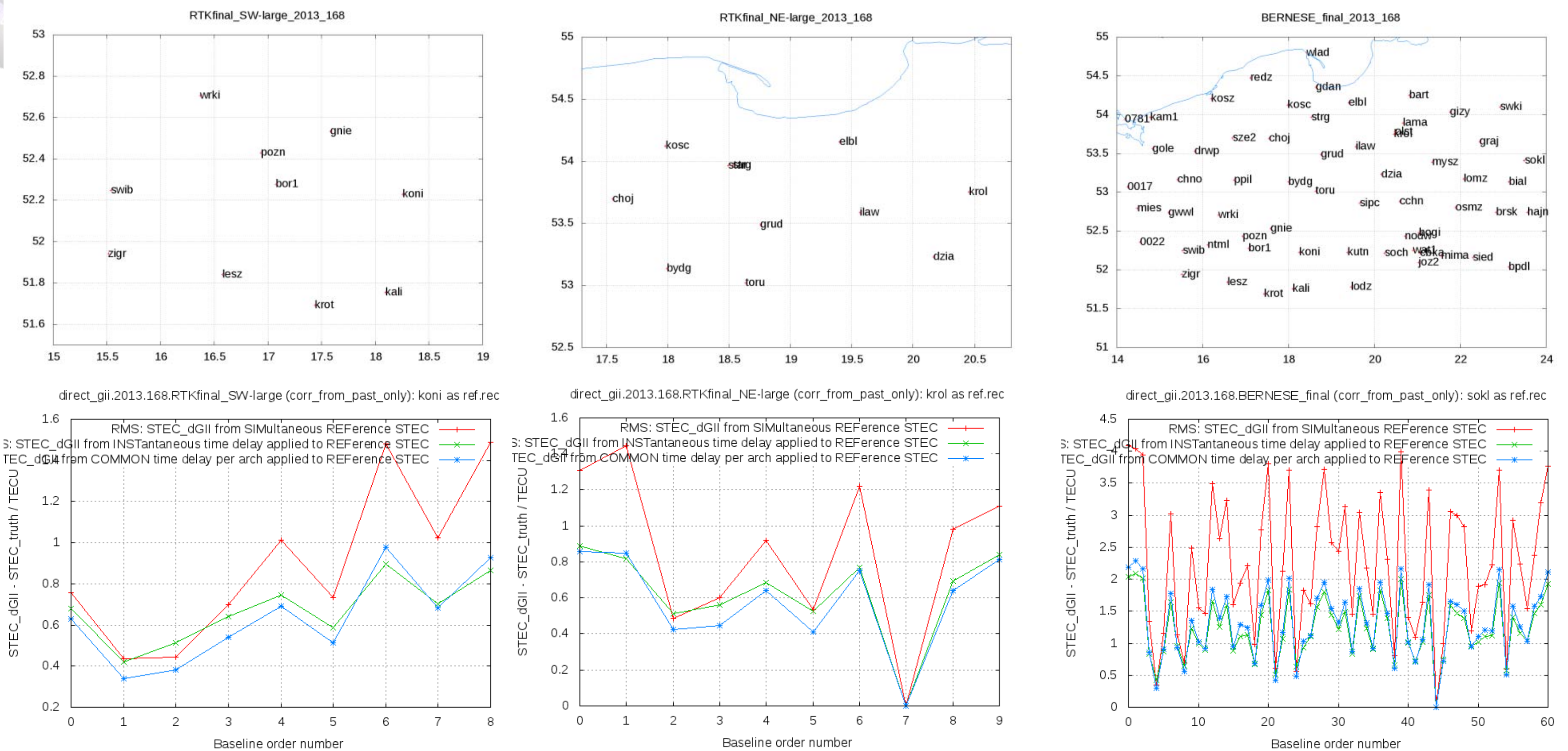


Map of dGII analyzed receivers in RTKfinal-SW-large (left), RTKfinal-NE-large (central) and BERNESE-final (right) networks, and corresponding performance of **dGII** for different baselines, **vs. no applying it** with eastern reference sites koni, krol and sokl, respectively (right column, Poland, summer day of 168, 2013).

# Positioning – ambiguity and coordinate domain 60-80 km baselines, summer day (168/2013)

**Red.RNX** **Mod.RNX+Prop.STEC**

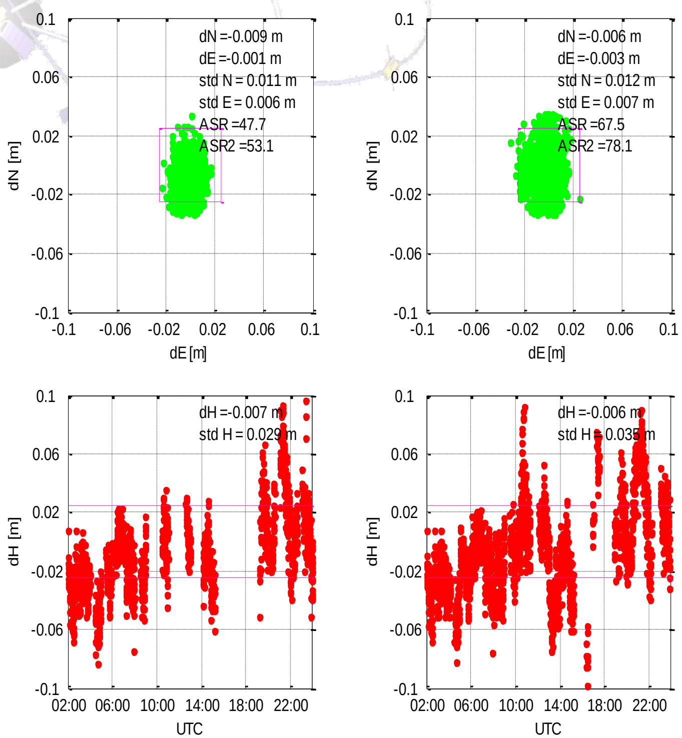


Fig. Baseline BOR1-KONI on 168 DOY (left panel – original observations, right panel – MSTID-corrected)

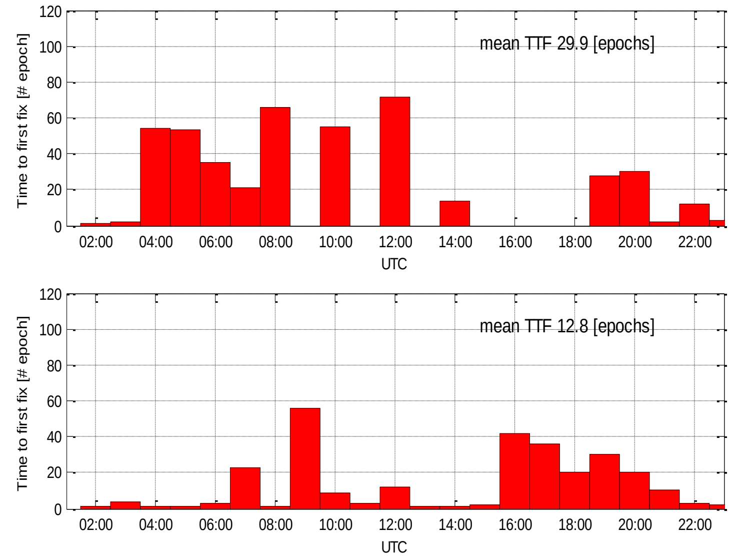


Fig. Time to fix, baseline BOR1-KONI on 168/2013 (top panel – original observations, bottom panel – MSTID-corrected)

| 168 DOY CWP net | | ASR [%] | TTFF [epochs] | N std [m] | E std [m] | U std [m] |
|---|---|---|---|---|---|---|
| **Baseline** | *strategy* | | | | | |
| **BOR1-KONI** | Original obs. | 53 | 29.9 | 0.011 | 0.006 | 0.029 |
| | MSTID-corrected | **78** | **12.8** | **0.012** | **0.007** | **0.035** |
| **GNIE-KONI** | Original obs | 74 | 18.3 | 0.013 | 0.008 | 0.025 |
| | MSTID-corrected | **83** | **15.7** | **0.013** | **0.009** | **0.036** |

**Improvement in the ambiguity resolution domain.**

# Improvement in the troposphere modeling

Original RINEX files:

smaller AR%, ZTD estimates close to EPN final solution

Reduced/modified RINEX files with MSTID dGII models:

small differences in WL and NL AR%, improvement in QIF AR% up to 14%

different ZTD estimates than using CODE iono model (but equal formal errors)

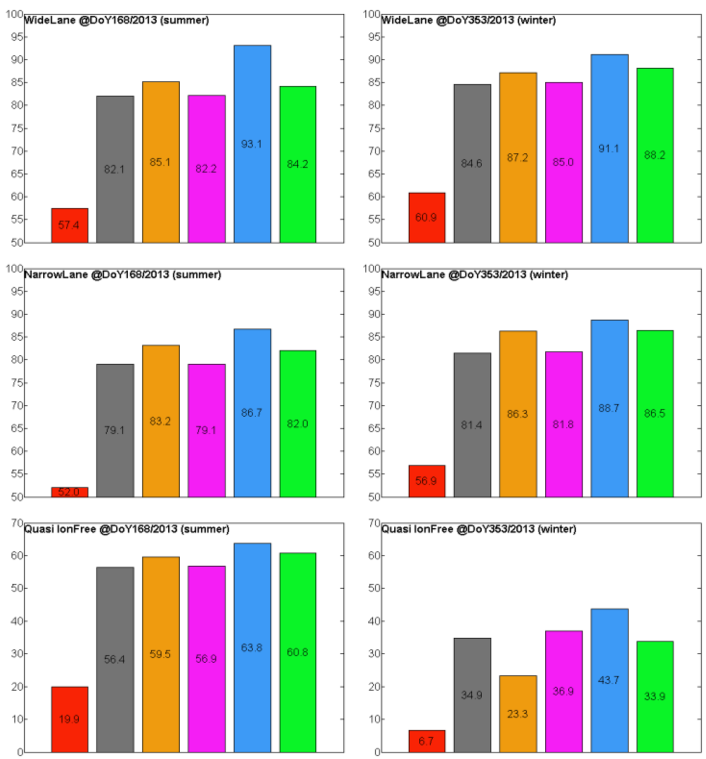


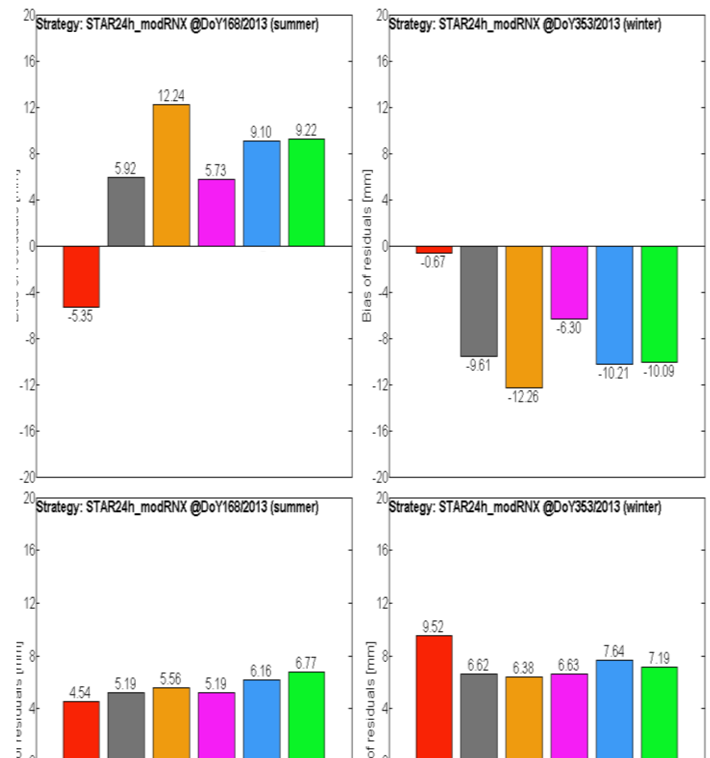


Org.RNX+CodeION
Red.RNX(noSTEC)
Red.RNX+CodeION
Mod.RNX(Sim.STEC)
Mod.RNX(Truth.STEC)
Mod.RNX(Prop.STEC)

# Conclusions

- Recent findings on the study of Solar Flares and MSTIDs with GNSS have been summarized as far as its applications
- GNSS proves again its versatility and power in order to become not only an extremely sensitive and accurate global ionospheric sounder but a calibrated solar observational instrument as well.

**Thank you**